

Molecular Spintronics: Spin-Dependent Electron Transport in Molecular Wires

Eldon G. Emberly¹ and George Kirczenow²

¹*NEC Research Institute, 4 Independence Way, Princeton, New Jersey 08540*

²*Department of Physics, Simon Fraser University, Burnaby, British Columbia, Canada, V5A 1S6*

(March 5, 2019)

Abstract

We present a theoretical study of spin-dependent transport through molecular wires bridging ferromagnetic metal nanocontacts. We extend to magnetic systems a recently proposed model that provides a *quantitative* explanation of the conductance measurements of Reed *et al.* [1] on Au break-junctions bridged by self-assembled molecular monolayers (SAMs) of 1,4-benzene-dithiolate (BDT) molecules. Based on our calculations, we predict that spin-valve behavior should be observable in nickel break-junctions bridged by SAM's formed from BDT. We also consider spin transport in systems consisting of a clean ferromagnetic nickel STM tip and SAMs of benzene-thiol molecules on gold and nickel substrates. We find that spin-valve behavior should be possible for the Ni substrate. For the case where the substrate is gold, we show that it should be possible to inject a highly spin-polarized current into the substrate.

I. INTRODUCTION

Over the past few years, molecular wires formed by bridging pairs of metallic contacts with organic molecules, have been shown to display a remarkable range of electron transport phenomena [1–7]. Some wires display rectification [3], others yield negative differential resistance [7], and still others involve molecules that are known to switch conformations and exhibit switching behavior in their transport characteristics [4]. As this special issue on electron transport will attest, understanding the measured experimental data is a great challenge that requires bringing together principles from both chemistry and physics. A wide variety of theoretical approaches have arisen over the past few years for the modeling of molecular wire systems. These range from self-consistent calculations [8–13] to semi-empirical methods [14–17]. Molecular wires have great promise from a pure science perspective and also potentially for applications. Hence both experimental and theoretical research in this field continues to attract increasing interest.

Another area of research that has also seen great growth over the past few years is spintronics, a branch of electronics that employs the electron's spin degree of freedom as well as its charge to store, process and transmit information [19–21]. Important spintronic phenomena include giant magnetoresistance, spin valve behavior and injection of spin polarized currents from ferromagnetic materials to paramagnetic materials [22–33]. The prototypical spin valve system consists of two ferromagnetic leads separated by a paramagnetic coupling layer. Transport is measured between the two ferromagnetic layers under an applied voltage. The system functions as a spin valve when it exhibits a difference in its electrical conductance between configurations in which the magnetizations of the ferromagnetic layers are aligned parallel and anti-parallel. Different materials can display very different spintronic properties. For example, injection of spin currents from metallic ferromagnets into non-magnetic metals is relatively straight forward and was first demonstrated experimentally more than a decade ago [24]. Since then it has found important practical applications in information storage technology [19]. However attempts at demonstrating efficient spin injection from ferromagnetic metals into semiconductors through solid state interfaces have encountered fundamental obstacles [29] and work is underway to determine whether these may be overcome through the use of potential barriers and/or interfaces that obey certain selection rules [29–33].

Much less is known at the present time about spin transport in molecules. There have been a few studies of spintronic systems involving carbon nanotubes [34,35]. However to our knowledge whether functioning self-assembled nanoscale spintronic devices can be made out of organic molecules and magnetic nanocontacts has not as yet been explored experimentally or theoretically. In this paper we show that spin-dependent transport phenomena should be readily observable in such molecular wire systems using currently available experimental techniques. We consider two classes of systems: break-junctions made from ferromagnetic nickel bridged by self-assembled monolayers of organic molecules, and STM setups consisting of a clean single-crystal nickel tip and a SAM on a gold or nickel (100) substrate. Schematics of these systems are shown in Fig. 1. Our calculations suggest that spin-valve effects and spin injection should be possible in these molecular wire based systems.

As a reference point for the present calculations, we briefly revisit a recently proposed model that has been instrumental in achieving a quantitative understanding [18] of current

flow in self-assembled molecular wires bridging a non-magnetic break-junction. In this model it is assumed that current flows not through a single molecule connecting the two tips of the metal break-junction as in previous theories, but through overlapping molecules, with each molecule chemically bonded to only one metal tip. This model together with a semi-empirical method for the solution of the transport problem is able to quantitatively reproduce [18] the measured conductance data of Reed *et al.* [1] for gold break junctions bridged by benzene-dithiol molecules. Because it is not compute-intensive, a semi-empirical theoretical approach allows us to calculate the transport properties of an ensemble of possible orientations of the overlapping molecules and to include the effects of positional disorder. Thus we are able to calculate transport properties averaged over configurations. We feel that the success of this work has demonstrated that semi-empirical methods are useful as a tool for evaluating and estimating effects that are not easily accessible to ab-initio techniques.

This paper is organized as follows: In Sec. II, we give a brief summary of a method for calculating the transport characteristics of a molecular wire. The current is evaluated via Landauer theory and the scattering problem is solved using a semi-empirical tight-binding form of Schroedinger's equation. Sec. III contains a summary of the model that we have proposed for understanding electrical conduction in non-magnetic metal break-junctions bridged by SAM's [18], and also representative results of calculations of the differential conductance of non-magnetic systems that are in quantitative agreement with experiment [1]. These results provide a useful benchmark for comparison with our calculations for magnetic systems that follow. Our spin-dependent transport results are presented in Sec. IV and V. In Sec. IV we consider molecular wires bridging magnetic break junctions. We predict that spin-valve behavior should be experimentally detectable in break-junction measurements on SAM's, where the break junction is made from ferromagnetic nickel. Sec. V details our results for systems that include magnetic STM tips. We show that spin-injection and spin-valve effects should be observable in the systems that we consider. Finally, in Sec. VI we present some conclusions that may be drawn from this work.

II. A METHOD FOR EVALUATING THE ELECTRICAL CURRENT IN MOLECULAR WIRES

In this section, we briefly review a method for calculating the conductance properties of a molecular wire system. We consider a molecular wire to consist of a pair of electrodes which act as a source and drain for electrons, that are connected by a molecule or molecules. A bias is applied to the electrodes and an electric current flows through the system. A standard method for evaluating the current in such a system is Landauer theory [36]. It relates the electric current flowing through the molecular conductor to the probability for a single electron to scatter from one electrode to the other. For a two-terminal system, the current as a function of the applied bias V can be calculated from the following equation

$$I(V) = \frac{e^2}{h} \int dE T(E, V) [F(E, \mu_S) - F(E, \mu_D)] \quad (1)$$

where $F(E, \mu)$ is the equilibrium Fermi distribution and $\mu_{S,D} = E_F \pm eV/2$ are the electrochemical potentials of the electrodes in terms of the common Fermi energy E_F of the source

(S) and drain (D) electrode respectively. The transmission probability $T(E, V)$ is the sum of the transmission probabilities for both spin up and spin down electrons to scatter through the system at energy E . For a thorough review of Landauer theory see Ref. [37].

A variety of methods exist for solving the scattering problem to determine the transmission probability. These range from self-consistent calculations based on density-functional theory [8–13], to simpler semi-empirical tight binding approaches [14–17]. The density-functional methods have the advantage of self-consistently calculating the effects of the electro-static potential that arises in the vicinity of the molecule due to the applied bias V and any charge transfer that may arise between the leads and the molecule. They have the disadvantage of being numerically intensive which restricts the size of the problems to which they can be applied at present. They constitute the present state of the art, but never-the-less they rely on approximations whose reliability for transport calculations is unknown when the system departs significantly from equilibrium, a case that is particularly important for molecular wire systems. Semi-empirical approaches do not include the effects of the electro-static field self-consistently. Many-body effects are included implicitly to a limited extent in the parameters, and the electro-static field may be added as an extra potential which can be used to approximate the true field. Because of the speed with which calculations using semi-empirical methods can be carried out, they have the advantage of being able to study much larger systems, including also the various changeable degrees of freedom that influence transport in these systems. They have been shown to produce quantitatively similar results to density functional calculations in the linear voltage regime for systems where the effects of the self-consistent potential are less significant [16,38,39]. Thus semi-empirical approaches should be considered as a valuable tool in that they are able to provide an efficient method by which to evaluate the importance of various factors which may contribute to the transport properties of the molecular wire of interest. With the important factors determined, more sophisticated approaches can then be used to gain more quantitative understanding. What follows is a summary of the semi-empirical tight-binding approach that we use in this work to solve the scattering problem.

We calculate the transmission probability by explicitly calculating the single electron scattering states. Our starting point is Schrödinger's equation

$$H|\Psi\rangle = E|\Psi\rangle \quad (2)$$

where $|\Psi\rangle$ is the single-particle scattering state at energy E and H is the Hamiltonian for the entire system. For a two terminal molecular wire, we consider H to have the form

$$H = H_L^0 + H_M^0 + H_R^0 + V_L + V_R + V_{ext} + V_{SCF} \quad (3)$$

where $H_{L,M,R}^0$ are the Hamiltonians for the isolated left lead (L), molecule (M) and right lead (R). The molecule is coupled to the leads via $V_{L,R}$ for the left and right leads respectively. V_{ext} is the external potential due to the applied bias, and V_{SCF} represents the self-consistent electro-static potential which depends upon the charge distribution in the system. (In what follows, we no longer consider this term, however a tight-binding method including this term is given in Ref. [12,13]). The scattering state $|\Psi\rangle$ can be written as $|\Psi\rangle = |\Psi_L\rangle + |\Psi_M\rangle + |\Psi_R\rangle$, with the following conditions

$$|\Psi_L\rangle = |\Phi_{+,L}^\alpha\rangle + \sum_{\alpha'} r_{\alpha',\alpha} |\Phi_{-,L}^{\alpha'}\rangle \quad (4)$$

$$|\Psi_M\rangle = \sum_i c_i |\phi_i\rangle \quad (5)$$

$$|\Psi_R\rangle = \sum_{\alpha'} t_{\alpha',\alpha} |\Phi_{+,R}^{\alpha'}\rangle \quad (6)$$

where $|\Phi_{\pm,L/R}^{\alpha'}\rangle$ is the α'^{th} mode at energy E in either the left or right leads, with the \pm denoting whether the state is a rightward or leftward propagating or evanescent mode. The α^{th} mode is always a rightward propagating mode. The $|\phi_i\rangle$ are the bound eigenstates of the isolated molecule. The $r_{\alpha',\alpha}$ and $t_{\alpha',\alpha}$ are the reflection and transmission coefficients respectively. The total transmission probability for an electron to go from the left lead to the right lead is given by

$$T(E, V) = \sum_{\alpha, \alpha'} \frac{v_{\alpha'}}{v_\alpha} |t_{\alpha',\alpha}|^2 \quad (7)$$

where the sum over α is over rightward propagating modes in the left lead and the sum over α' is over rightward propagating modes in the right lead; all modes at energy E . If the system is magnetic, we assume the effects of spin orbit coupling on transport through the molecular wire to be negligible [40] and solve for $T(E, V)$ for the spin up and spin down electrons separately.

We solve the above problem by representing the scattering states using a linear combination of atomic orbitals (LCAO) (also known as the tight-binding approximation) [43]. This yields a matrix form of Eqn. 2

$$\sum_j H_{ij} \Psi_j = E \sum_j S_{ij} \Psi_j \quad (8)$$

where H_{ij} is the Hamiltonian matrix in the chosen atomic orbital basis. If the basis of atomic orbitals is non-orthogonal then the non-diagonal elements of the overlap matrix S_{ij} must be included; an exact and easily implemented way to take them into account in molecular transport calculations is described in Ref. [44,45] Eq. 8 is a linear system which can be solved in a straightforward manner for the unknowns $r_{\alpha',\alpha}$, c_i , and $t_{\alpha',\alpha}$. The various propagating and evanescent modes in the leads are determined using standard transfer matrix methods.

We will use this method to explore spin transport in systems that include ferromagnetic leads below. However, we first discuss our model in the simpler context of a non-magnetic system for which it provides a quantitative explanation of available experimental data. This discussion will serve as a theoretical and experimental benchmark that will be helpful in understanding the predictions for magnetic systems that will follow.

III. TRANSPORT IN NON-MAGNETIC METAL BREAK-JUNCTIONS BRIDGED BY SELF-ASSEMBLED MONOLAYERS OF ORGANIC MOLECULES

In this section, we present a summary of a model [18] which can quantitatively account for the data measured by Reed *et al.* [1] on a gold break-junction bridged by self-assembled

monolayers (SAMs) of 1,4 benzene-dithiolate (BDT). Measurements on this system at room temperature displayed an apparently insulating region for bias values between approximately -0.7 and 0.7 volts, nearly symmetric differential conductance in the range from -4 to +4 volts and some asymmetry at higher bias. The measured conductance was much lower than the quantum $2e^2/h = (1/12.9k \text{ ohm})$ that sets the conductance scale for single-channel metallic nanowires and also much lower than the calculated conductances of molecular wires in which a single BDT molecule bridges the gap between the two contacts [38,16,9,17]; the first experimental conductance plateau occurred at a resistance of 22M ohm.

In the present model, instead of a single molecule chemically bonding to both leads, we consider the situation where each molecule bonds to only one metal tip and the current flows through overlapping molecules from one lead to the other. It has been previously shown theoretically, that having neighboring molecules through which the current can flow can have important consequences [46,47]. The present model accounts for the observed low conductance [1] as a result of the weak electrical coupling between the two overlapping molecules even though there is strong coupling between each molecule and the lead to which it is attached. It can also account for the observed reproducibility of the measurements [1] after repeated separation of the two tips: no chemical bonds are formed between the overlapping molecules or between the two leads, hence the SAM's can be pulled apart and brought back together reversibly. Regarding the observed symmetric behavior of the differential conductance [1], we argue that this symmetry arises from the system having the ability to sample all possible energetically favorable configurations of the overlapping molecules. Hence even though a given configuration of the two molecules may be asymmetric, because of thermal fluctuations the mirror configuration will also be sampled. Hence the average over the transport properties of all configurations yields a symmetric result, the small residual asymmetry of the current voltage characteristic in the experiment [1] being due to differences between the atomic structures of the two tips.

Fig. 1a is a schematic of the model we consider. Since both tips are densely coated with molecules we assume that molecules bonded to one tip can not also bond to the other. Because of this, the ends of the molecules that do not bond chemically to a gold surface remain as thiols (SH). For simplicity we consider the case where the current is carried predominantly through only a single pair of overlapping molecules. We argue that on average the faces of the two benzene rings should be oriented perpendicularly to each other because of electrostatic effects. The rings of carbons in similar molecules have been shown to have negative charge on their sides, whereas the hydrogens all have positive charge [48]. Thus a favorable configuration of two rings which minimizes the electrostatic energy should be one in which they are oriented perpendicularly to each other; this has been found to give rise to herring-bone patterns in molecular dynamics simulations of SAM's of benzene-thiol and similar molecules on gold [48]. Fig. 1a shows a possible configuration, where each molecule is bonded to the end of one tip and the molecules orient themselves to avoid steric clashes and minimize the electrostatic forces between them.

We simulate the above system by representing the break-junction using gold clusters to which we attach two BDT molecules. The gold clusters are in the [100] direction and consist of 5x5, 4x4, 3x3, and 2x2 layers of atoms, forming 54 atom clusters which form the tips of the metal break-junction. We only use the gold 6s orbital as we have found that including all of the orbitals (6s,6p,5d) yields quantitatively similar results for the bonding

geometries considered here. The BDT molecule consists of a benzene ring with the 1 and 4 hydrogens replaced with sulfur atoms. The sulfur atom that is not bonded to a lead remains a thiol. The sulfur atoms that bond to the gold are positioned over a four-fold hollow site 2 Angstroms from the ends of the gold clusters [49]. We use the standard extended Hückel parameters [50] to represent the valence orbitals of each atom in the system, and evaluate the necessary site energies, hopping energies and overlaps that make up the Hamiltonian and overlap matrices that go into the solution of Schrödinger's equation, Eq. 2. We attach to this molecular junction, semi-infinite 6x6 simple cubic multi-mode leads to act as source and drain. Each atom in the lead is simulated using just a single gold-like s orbital. We include disorder by randomly displacing each atom in the gold clusters by a distance consistent with the Debye-waller factor for gold. For the BDT molecule, we consider random displacements of each atom in the plane of the ring. We do this to approximate the vibrational disorder that will be present in the above systems at room temperature. For the overlapping ring system, we consider one molecule to assume a random tilt angle (between 20 and 40 degrees) with respect to the normal from the gold surface and then orient the second BDT molecule so that its ring is oriented perpendicular to the first, allowing for 20 degree fluctuations. We impose steric constraints by demanding that the atoms of the two BDT molecules be separated by distances ≥ 3 Angstroms. The transmission probability shown below is the average of transmission probabilities from 50 different atomic configurations.

In Fig. 2a, the average transmission probability is shown as a function of incident electron energy. There are several broad resonances. These resonances are due to highly hybridized molecule/gold states, with the resonances below -10 eV being due to the molecular HOMO states and those above -9 eV arising from the LUMO states. The resonances at -8.2 eV are due to the LUMO π^* state which is localized on the benzene ring. The multiple resonances at the LUMO are due not only to vibrational disorder but also to the fact that the wave function overlap between the two molecules results in a splitting of the almost degenerate LUMO levels. In the limit of averaging over an infinite number of configurations these peaks would smear into one broad peak [51].

Fig. 2b shows the calculated differential conductance at room temperature for the case of overlapping molecules using a Fermi energy for the gold leads of -10 eV. The first rise in conductance is due to resonant transmission between the HOMO of the molecules. The 2nd rise can be attributed to transmission between the LUMO state and also the lower HOMO state. The qualitative and quantitative agreement with the experimental data [1] in the voltage range below 2 volts is quite striking. The features in the calculated differential conductance curve appear at nearly the same values of the bias as in the experimental data, and also the magnitude of the calculated conductance is close to that which was observed in the experiment. Above 2 volts the qualitative agreement is less striking, yet the overall magnitude is in quantitative agreement with the measured values. In the non-linear regime the effects of electro-static potential are undoubtedly important and contribute to the shifting of the molecular orbitals. This would lead to shifting of the resonances shown in Fig. 2a. We have attempted to address qualitatively what this shifting may look like by introducing potential drops at the contacts between the leads and molecules as well as in between the two molecules. We assumed that 75% of the voltage drops between the two molecules while the other 25% drops at the metal contacts (this is a simple assumption which may or may not reflect the true potential profile of the system). We found that the resonances do

shift somewhat but that the overall magnitude of the resonances does not change appreciably. To obtain more accurate results at these higher biases, more sophisticated approaches which are based on density-functional theory should be used. Other improvements might be to use monte-carlo techniques to achieve a proper Boltzmann sampling of the possible configurations of the two molecules.

IV. SPIN VALVE BEHAVIOR IN A FERROMAGNETIC BREAK-JUNCTION BRIDGED BY SELF-ASSEMBLED MONOLAYERS OF AN ORGANIC MOLECULE

In this section we explore the transport properties of a break-junction bridged by SAMs of organic molecules where the break-junction is made of ferromagnetic nickel. Ferromagnets bridged by conducting layers are of interest from a device standpoint in part because of the possibility of spin-valve behavior. A spin-valve is characterized by a change in the conductance of the system when the magnetizations of the two ferromagnetic layers switch between parallel and anti-parallel configurations.

To gain some intuitive insight into this behavior, it helps to consider the simplified band structure of ferromagnetic nickel shown schematically in Fig. 3. Nickel is a ferromagnet because it has unequal spin up and spin down populations. The d-band for spin up electrons is completely filled, while for spin down electrons it is partially filled. This gives nickel a net spin which implies a net magnetization even in zero applied magnetic field. Now consider an experiment that measures the conductance between two nickel layers. In the situation where the two layers have their magnetizations aligned parallel, spin down electrons at the Fermi energy in the d-band of one layer will be transported into both the d-band and the s-band of spin down electrons of the other layer (ignoring spin-flip scattering and assuming that there is a conducting channel between the two layers). Then consider the situation where the magnetizations are aligned anti-parallel. Now the spin down electrons at the Fermi level in the d-band of one layer will be transported into the s-band of the spin up electrons of the other layer, since there is no d-band for spin up electrons in the drain at the Fermi energy. This simple argument implies that the band mismatch in the antiparallel configuration will lead to a different conductance. Hence one might expect a difference in conductance between the two configurations. Non-magnetic metals, thin insulating layers and vacuum tunnel barriers are among the systems that have been used successfully as conduits between ferromagnetic metal layers in such spin valve experiments. Here we consider the conduit to consist of self-assembled monolayers of organic molecules.

The structure of the system we consider is similar to that of the system studied in the preceding section but here the nanoscale contacts are of (100) nickel. Again they are in the form of clusters built from 5x5, 4x4, 3x3 and 2x2 layers of atoms. We also make the assumption that each cluster forms a single magnetic domain. We again consider BDT to be the molecule forming the SAM on each tip. We assume that each sulfur atom that binds to a tip is situated 1.7 Angstroms above a four-fold site of nickel. The tight-binding parameters that we use for nickel's 4s,4p and 3d orbitals are taken from Ref. [52] for bulk ferromagnetic nickel. There are two sets of parameters, one for spin up electrons and one for spin down electrons. The parameters for the atoms making up the molecules are taken from the

standard extended Hückel set [50]. We evaluate the Hamiltonian matrix elements coupling the nickel tips to the molecules using extended Hückel where now the Ni parameters are the standard ones used in extended Hückel calculations [50]. Thus we make the assumption that spin down and spin up electrons interact in the same manner with the molecule. The energy scale used in Ref. [52] is offset relative to that used in extended Hückel theory. Thus to achieve consistency between the two schemes we added a constant $\epsilon = -17.2$ eV to all of the site energies taken from Ref. [52] and also adjusted the off-diagonal Hamiltonian matrix elements accordingly (for further details of this procedure see the Appendix). (The shift was calculated by aligning the Fermi energies: $E_F = 8.7$ eV from Papaconstantopoulos and $E_F = -8.5$ eV for bulk Ni as calculated from the parameters used by extended Hückel). Again, 6x6 simple cubic semi-infinite ideal leads were coupled to the last layer of each cluster.

We performed transport calculations for the cases where the magnetizations of the single domain tips are aligned parallel and anti-parallel. The transmission probabilities for these two cases are shown in Fig. 4. Because the dimensionality of the Hamiltonian matrix has grown nine fold over the case where the tips were made of gold, we did not perform averaging over the orientations of the two molecules – what is shown is $T(E)$ for only one particular configuration. (Our purpose here is not so much to make quantitative predictions, but simply to use the semi-empirical approach to gain insight into what might be observed since, as was shown in the preceding section, calculations such as this can make reasonable assessments about the magnitude of transmission and also the hybridization that occurs between the molecules and the metal). Fig. 4a shows the total transmission for the case where the tips' magnetizations are aligned parallel. Two calculations were performed to generate this curve. The first involved calculating $T_{down}(E)$ for the system where spin down parameters are used on both tips, and then secondly calculating $T_{up}(E)$ for the case where spin up parameters are used on both tips. The total transmission is then $T(E) = T_{up}(E) + T_{down}(E)$. Above -8.5 eV, the dominant channel in Ni is s-type, and hence $T(E)$ displays similar features to those seen for the gold break-junction system: There is a resonance at -8.2 eV from the LUMO and a broader peak at higher energy from the next LUMO. Below -8.5 eV we see the effects of the d-states of Ni. The HOMO and LUMO hybridize with the d-states of Ni near the Fermi energy to form transporting states throughout the nominal HOMO-LUMO gap of the molecule. Fig. 4b shows $T(E)$ for the case where the tips are aligned anti-parallel. This curve was calculated by using spin down parameters on one tip and spin up parameters on the other. This yields $T_{down \rightarrow up}(E)$ and due to detailed balance the total transmission is $T(E) = 2T_{down \rightarrow up}(E)$. Because of the band mismatch, there are some differences between the parallel and antiparallel configurations. The first resonance below -8.5 eV is clearly lower in amplitude for the case where the spins are aligned anti-parallel compared to the parallel case. This should manifest itself as a difference in conductance between these two configurations.

In Fig. 5 we show the calculated differential conductance for the break-junction system at room temperature using a Fermi energy of -8.5 eV. The solid line corresponds to the case where the two tips have their magnetizations aligned parallel. One might imagine separating the tips and applying a magnetic field so as to flip the spin on one of the tips. Alternatively the break junction may be fabricated so that the Ni film on one side of the break junction is thinner than on the other; the magnetization of the thinner film will reverse at a lower applied magnetic field than that of the thicker film. The dashed line

shows the differential conductance for the situation where the tips are aligned anti-parallel. The difference in conductance is not dramatic, although it should be within the realm of experimental detection. Thus this simple model suggests that spin valve behavior should be observable in a break-junction measurement. We are currently exploring what the effect of averaging over more orientations of the two molecules has on the calculated differential conductance.

V. SPIN DEPENDENT TRANSPORT IN STM MEASUREMENTS ON ORGANIC MOLECULES

In this section we consider some possible experiments which utilize STM apparatus with an STM tip made from single crystal nickel with a single magnetic domain. Specifically we consider two systems: one with a SAM grown on a substrate of gold and secondly one where the SAM is grown on nickel. We consider the SAM to be made from benzene-thiol (BT), where the thiol binds to the substrate. The end of this molecule that does not carry the thiol group should not bond chemically to the Ni STM tip, and we will assume that the tip is clean, i.e., free from adsorbed molecules. For the system with the gold substrate we assume the possibility of detecting any spin-polarized current that may be injected into it from the STM tip. For the case where the substrate is nickel, we are again interested in the possibility of spin-valve behavior.

Fig. 1b is a schematic of the set up that we consider. The substrate is taken to consist of (100) metal, and we model it using 5x5, 6x6, 5x5, and 6x6 layers of atoms which form a 122 atom cluster. The tip is taken also to be in the [100] direction, and consists of 5x5, 4x4, 3x3, 2x2 layers of atoms which are capped with a single atom. The molecule is assumed to be perpendicular to the surface with the sulfur atom situated over a four-fold hollow site on the substrate. For the case where the substrate is gold we assume a binding distance of 2 Angstroms, and when it is nickel, a distance of 1.7 Angstroms. We assume that the STM tip is situated over the principal axis of the molecule at a distance of 2 Angstroms from the end hydrogen atom. We only use the 6s orbital for the gold atoms and take the parameters from extended Hückel.

In the case where both the substrate and STM tip are Ni we again use Papaconstantopoulos' [52] parameters for both the spin up and spin down bands adjusted for consistency with the molecular extended Hückel parameters as was discussed in Sec. IV. In the case where the STM tip is Ni and the substrate is gold it is necessary to address the further complication that although the tip and substrate are of different metals, the Fermi levels (or, in more precise terms, the electro-chemical potentials) of the tip and substrate must be equal at zero bias if the two metals are in electrical contact with each other through the molecular wire. (If their Fermi levels were not aligned at zero bias then an electric current would flow until an equilibrium state were reached in which the electrostatic potential due to the charge transferred between the two metals would align their Fermi levels and the current would cease to flow.) This Fermi level alignment is taken into account in our calculation by applying an equal shift to the site energies and Fermi level of Ni given in Ref. [52], the shift (-18.7 eV) being chosen so as to align the Fermi level of Ni to the Fermi level for gold (-10 eV) obtained using the extended Hückel parameters. Again the off-diagonal matrix

elements of the tight-binding Hamiltonian for Ni are adjusted accordingly. We treat the molecule using extended Hückel. As was done previously for the Ni break-junction system, the coupling parameters between Ni and molecule are evaluated using extended Hückel.

Transmission probabilities for the situation where the substrate is gold are shown in Fig. 6. Fig. 6a is for the case where the STM tip is made of gold; we include it as a reference for comparison with our results for the more complicated magnetic case where the STM tip is made of nickel. The features seen in $T(E)$ in Fig. 6a are qualitatively similar to what was seen for the break-junction system. The resonances around -8 eV are due to the LUMO's of BT. There is a resonance near -10.6 eV which is due to the HOMO. The resonances in between -8 and -10.6 eV can be attributed to tunneling into the molecule from sharp peaks in the density of states of the STM tip.

The calculated $T(E)$ for the case where the tip is made of Ni are shown in Fig. 6b,c: (b) shows $T_{down}(E)$ for the spin down electrons. (c) shows $T_{up}(E)$ for the spin up electrons. Again, the d-states from the Ni hybridize with the molecular states to provide channels for transport. There are striking differences between the two curves below -10 eV (the adjusted Fermi energy of the Ni tip). Because the spin down d-band straddles the Fermi energy there are d-state resonances near -10 eV. For the spin up electrons, the d-band begins about 1 eV below this, and so no spin up d-states contribute to transport within this window of energy. Because of this difference, there is a net difference between the number of spin down versus spin up electrons transmitted into the substrate. This generates a non-equilibrium population of spin states in the s-band of the gold substrate. To quantify this difference we have calculated the current due to spin up and spin down electrons in this system as a function of applied bias. This is shown in Fig. 7. The spin down current is greater than the spin up current by a factor of approximately five. Thus a strong spin polarization of the current should be expected in this system.

The last case that we consider is that where both the tip and substrate are made of nickel. Here, we are again interested in whether spin-valve behavior should be observable. Since the only metal present in the system is Ni we revert to the tight binding and Fermi energy parameters that were described in Sec. IV. The transmission probability for this system where the magnetizations of the substrate and tip are aligned parallel and anti-parallel are shown in Fig. 8(a) and (b) respectively. For the parallel case there is a resonance near -8.7 eV which does not appear for the case where the magnetizations are antiparallel. This should manifest itself as a noticeable difference in differential conductance. Fig. 9 shows the calculated differential conductance at room temperature, again using a Fermi energy of -8.5 eV for nickel [53]. The spin valve effect is now more prominent than that predicted for the break-junction system. The first rise in conductance for the parallel aligned configuration is due to transport through the state at -8.7 eV. This state does not exist in the anti-aligned configuration, and so there is no significant rise in conductance for that situation. The difference in conductance between the two cases is now a factor of two, which should be readily detectable.

VI. CONCLUSIONS

In conclusion, we have shown that spin-dependent transport should be readily observable in molecular wire systems. First, we gave a summary of a model of electrical conduction through self-assembled molecular mono-layers that bridge metal break-junctions [18]. We assumed that current flows through overlapping molecules each of which is chemically bonded to only one tip. We showed that this model can quantitatively and qualitatively reproduce the experimental data reported by Reed *et al.* [1] for a non-magnetic system. Using this model, we then proceeded to show that it should be possible to observe spin-valve behavior in a break-junction formed from ferromagnetic nickel and bridged by SAM's of 1,4 benzene-dithiol. The spin-valve behaviour occurs because of band mismatch between the two ferromagnetic leads, with the molecules providing transporting states between the two leads. The second class of systems we considered was a variety of STM configurations, with the STM tip made from single-crystal and single-domain nickel. We showed that it should be possible to inject a highly spin-polarized current into a gold substrate which has a self-assembled monolayer of benzene-thiol on it. Lastly, we showed that spin-valve behavior should be detectable if the substrate is nickel covered by a SAM of benzene-thiol. We found that the STM set-up produced a larger spin valve effect than the break-junction system. These calculations show that semi-empirical transport methods can be useful in exploring phenomenology of molecular wires, and yield results that should be helpful in understanding which effects play an important role in governing electron transport.

We would like to thank Ross Hill, Bret Heinrich, and Alistair Rowe for rewarding discussions and helpful suggestions. This work was supported by NSERC and by the Canadian Institute for Advanced Research.

VII. APPENDIX

Here we review how to change the Hamiltonian matrix elements when the energy is rescaled and a constant energy shift is added to the scattering problem for the case where the underlying basis is non-orthogonal. Schroedinger's equation for the scattering problem is $H|\Psi\rangle = E|\Psi\rangle$. We can scale this equation by a factor c , and add and subtract a constant energy shift ϵ yielding

$$cH|\Psi\rangle = cE|\Psi\rangle + \epsilon|\Psi\rangle - \epsilon|\Psi\rangle. \quad (9)$$

We redefine the scattering energy to be $E' = cE - \epsilon$. Using a non-orthogonal basis the above equation becomes a matrix equation,

$$\sum_j (cH_{ij} - \epsilon S_{ij}) \Psi_j = E' \sum_j S_{ij} \Psi_j. \quad (10)$$

We can define a new Hamiltonian matrix after the application of a scaling and a constant energy shift by

$$H'_{ij} = cH_{ij} - \epsilon S_{ij}. \quad (11)$$

Thus we see that not only are the diagonal elements changed by the shift, but also the off-diagonal elements when the basis is non-orthogonal.

REFERENCES

- [1] M. A. Reed, C. Zhou, C. J. Muller, T. P. Burgin, and J. M. Tour, *Science* **278**, 252 (1997).
- [2] S. Datta, W. Tian, S. Hong, R. Reifenberger, J. I. Henderson, C. P. Kubiak, *Phys. Rev. Lett.* **79**, 2530 (1997).
- [3] R. M. Metzger, B. Chen and M. P. Cava, *Thin Solid Films* **327/329**, 326 (1998).
- [4] C. P. Collier, G. Mattersteig, E. W. Wong, Y. Luo, K. Beverly, J. Sampaio, F. M. Raymo, J. F. Stoddart and J. R. Heath, *Science* **289**, 1172 (2000).
- [5] J. K. Gimzewski and C. Joachim, *Science* **283**, 1683 (1999).
- [6] J. Reichert, R. Ochs, D. Beckman, H. B. Weber, M. Mayor and H. v. Löhneysen, *cond-mat/0106219* (2001).
- [7] J. Chen, M. A. Reed, A. M. Rawlett and J. M. Tour, *Science* **286**, 1550 (1999).
- [8] N. D. Lang and P. Avouris, *Phys. Rev. Lett.* **81**, 3515 (1998).
- [9] M. Di Ventra, S. T. Pantelides, and N. D. Lang, *Phys. Rev. Lett.* **84**, 979 (2000).
- [10] J. Taylor, H. Guo, J. Wang, *Phys. Rev. B* **63**, 121104 (2001).
- [11] V. Mujica, A. E. Roitberg and M. Ratner, *J. Chem. Phys.* **112**, 6834 (2000).
- [12] E. Emberly and G. Kirczenow, *Phys. Rev. B* **62**, 10451 (2000).
- [13] E. Emberly and G. Kirczenow, *Phys. Rev. B* **64**, 125318 (2001).
- [14] M. Magoga, and C. Joachim, *Phys. Rev. B* **56**, 4722 (1997).
- [15] S. N. Yaliraki, M. Kemp, and M. A. Ratner, *Jnl. Am. Chem. Soc.* **121**, 3428 (1999).
- [16] E. Emberly and G. Kirczenow, *Phys. Rev. B* **58**, 10911 (1998).
- [17] L. E. Hall, J. R. Reimers, N. S. Hush and K. Silverbrook, *J. Chem. Phys.* **112**, 1510 (2000).
- [18] E. G. Emberly and G. Kirczenow, *Phys. Rev. B* (2001).
- [19] G.A. Prinz, *Physics Today* **45**, 58 (1995); *Science* **282**, 1660 (1998)
- [20] J. M. Kikkawa, *Physics Today* **52**, 33 (1999).
- [21] S. Datta and B. Das, *Appl. Phys. Lett.* **56**, 665, (1990).
- [22] R. Meservey, P. M. Tedrow and P. Fulde, *Phys. Rev. Lett.* **25**, 1270 (1970).
- [23] M. Julliere, *Phys. Lett.* **54A**, 225 (1975).
- [24] M. Johnson and R. H. Silsbee, *Phys. Rev. Lett.* **55**, 1790 (1985).
- [25] M. N. Baibich, J. M. Broto, A. Fert, F. Nguyen Van Dau, and F. Petroff P. Etienne, G. Creuzet, A. Friederich, and J. Chazelas, *Phys. Rev. Lett.* **61**, 2472 (1988)
- [26] S.F. Alvarado, P. Renaud, *Phys. Rev. Lett.* **68**, 1387 (1992)
- [27] R. Fiederling, M. Keim, G. Reuscher, W. Ossau, G. Schmidt, A. Waag, L. Molenkamp, *Nature* **402**, 787 (1999).
- [28] Y. Ohno, D. K. Young, B. Beschoten, F. Matsukura, H. Ohno and D. D. Awschalom, *Nature* **402**, 790 (1999).
- [29] G. Schmidt, D. Ferrand, L. W. Molenkamp, A. T. Filip, and B. J. van Wees, *Phys. Rev. B* **62**, R4790 (2000).
- [30] E. I. Rashba, *Phys. Rev. B* **62**, 16267 (2000).
- [31] G. Kirczenow, *Phys. Rev. B* **63**, 54422 (2001).
- [32] V. P. LaBella, D. W. Bullock, Z. Ding, C. Emergy, A. Venkatesen, W. F. Oliver, G. J. Salamo, P. M. Thibado, and M. Mortazavi, *Science* **292**, 1518 (2001).

[33] H.J. Zhu, M. Ramsteiner, H. Kostial, M. Wassermeier, H.P. Schönherr, K.H. Ploog, Phys. Rev. Lett. **87**, 16601 (2001)

[34] K. Tsukagoshi, B. W. Alphenaar, and H. Ago, Nature (London) 401, 572 (1999).

[35] H. Mehrez, J. Taylor, H. Guo, J. Wang and C. Roland, Phys. Rev. Lett. **84**, 2682 (2000).

[36] R. Landauer, IBM J. Res. Dev. **1**, 223 (1957); R. Landauer, Phys. Lett. **85A**, 91 (1981).

[37] For a comprehensive review of Landauer-Büttiker theory see S. Datta, *Electronic Transport in Mesoscopic Systems*, Cambridge University Press, Cambridge (1995).

[38] Extended Hückel calculations of transport through BDT/Au systems have also been reported by S. Datta and collaborators (unpublished).

[39] E. Emberly and G. Kirczenow, Phys. Rev. B **60**, 6028 (1999).

[40] In certain semiconductor systems it is expected that spin-orbit coupling should give rise to interesting spin transport phenomena [21,41] through the Rashba mechanism [42], however in this work we are concerned with small molecules consisting of relatively light atoms that are not expected to exhibit pronounced spin-orbit-related transport effects.

[41] F. Mireles and G. Kirczenow, Phys. Rev. B **64**, 24426 (2001)

[42] Y. A. Bychkov E. I. Rashba, J. Phys, C **17**, 6039 (1984).

[43] S. P. McGlynn, L. G. Vanquickenborne, M. Kinoshita and D. G. Carroll, see chap. 3 of “Introduction to Applied Quantum Chemistry”, Holt, Reinhart and Winston, Inc. (1972).

[44] E. G. Emberly and G. Kirczenow, Phys. Rev. Lett. **81**, 5205 (1998).

[45] E. G. Emberly and G. Kirczenow, Journal of Physics Condensed Matter **11**, 6911 (1999).

[46] S. N. Yaliraki, M. A. Ratner, J. Chem. Phys. **109**, 5036 (1998).

[47] N. D. Lang and Ph. Avouris, Phys. Rev. B **62**, 7325 (2000).

[48] H. H. Jung, Y. D. Won, S. Shin and K. Kim, Langmuir **15**, 1147 (1999).

[49] H. Sellers, A. Ulman, Y. Schnidman and J. E. Eilers, J. Am. Chem. Soc. **115**, 9389 (1993).

[50] S. Alvarez, “Table of Parameters for Extended Hückel Calculations”, (1985).

[51] We found that the transmission probability was larger for the energetically unfavorable configuration where the two molecules are aligned parallel compared to the more favorable perpendicular alignment.

[52] D. A. Papaconstantopoulos, *Handbook of the Band Structure of Elemental Solids* (Plenum Press, 1986)

[53] We have assumed symmetric drops in potential at the two metal-molecule interfaces in the Landauer formula, and have not calculated $T(E)$ at higher applied biases. However, the system is asymmetrically coupled and therefore some asymmetry in dI/dV may be expected to be observed experimentally as the STM tip is retracted from the molecule and the asymmetry between the couplings at the two molecule-metal interfaces becomes more pronounced.

FIGURES

FIG. 1. Schematic of two molecular wire configurations. (a) Metal break-junction bridged by self-assembled monolayers of organic molecules. (b) Clean STM tip approaches a self-assembled molecular monolayer of organic molecules on a metal substrate.

FIG. 2. (a) Calculated average transmission probability at zero applied bias over 50 different atomic configurations for the system shown in Fig. 1a, where the break-junction is made of gold. (b) Calculated differential conductance at room temperature using a Fermi energy of the gold leads of -10 eV.

FIG. 3. Simplified schematic of the band structure of ferromagnetic nickel. On the left, the band structure of spin down electrons. The d-band is partly empty. On the right, the band structure for the spin up electrons. Here, the d-band is completely occupied. The 0.54e hole in the d-band of the spin down electrons gives Nickel a net magnetic moment of $0.54\mu_B$.

FIG. 4. Transport properties for a single configuration of an overlapping pair of BDT molecules bonded to a Ni break-junction. (a) Total transmission probability for the case where the magnetizations on the left and right leads are aligned parallel. (b) Total transmission probability for the case where the magnetizations are aligned anti-parallel. The vertical line indicates the chosen Fermi energy for the nickel leads of -8.5 eV (see text).

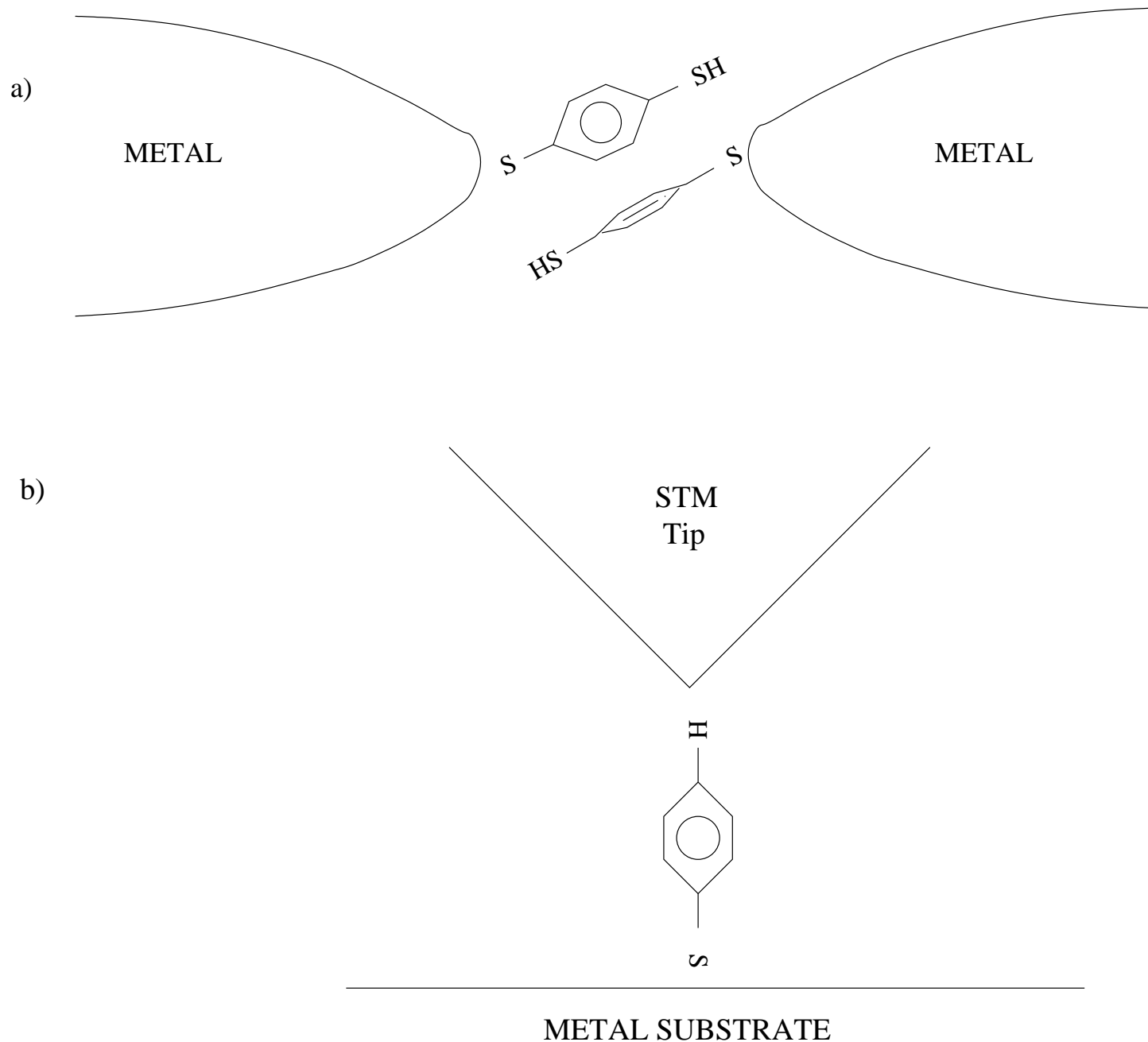
FIG. 5. Calculated differential conductances of the Ni-BDT break-junction system at room temperature using a Fermi energy of -8.5 eV. (Solid line) case where the magnetizations of the two tips are aligned parallel. (Dashed line) case where the magnetizations are aligned anti-parallel.

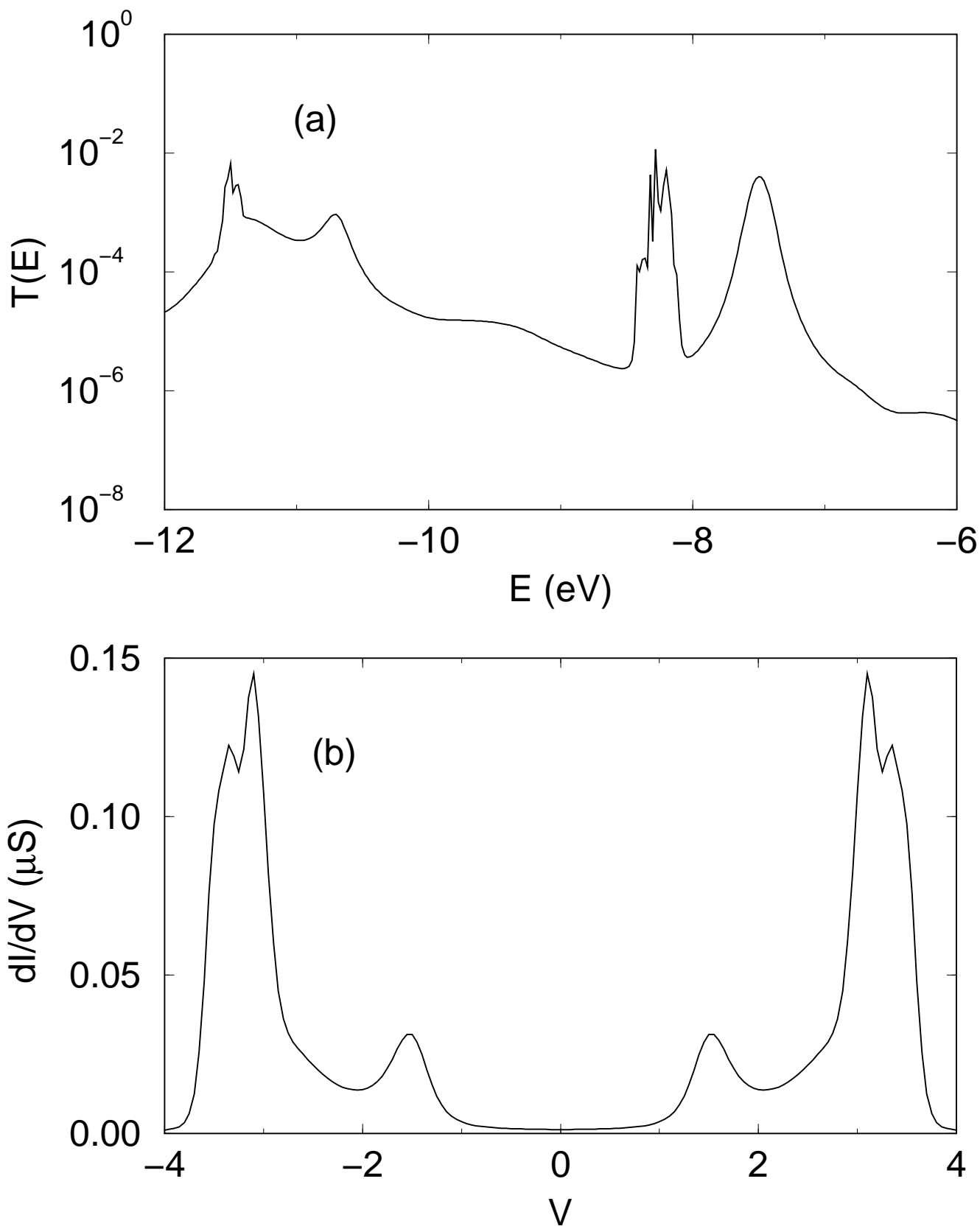
FIG. 6. Transmission probabilities for the STM set-up using a gold substrate and benzene-thiol as the molecular wire. (a) case where the STM is gold. (b) Transmission probability for spin down electrons for the Ni tip. (c) Transmission probability for spin up electrons for the Ni tip.

FIG. 7. Calculated current at room temperature as a function of applied bias for the Ni STM tip - BT - Au substrate system. (Solid line) current due to spin down electrons. (Dashed line) current due to spin up electrons.

FIG. 8. Transmission probabilities for the case where the substrate is nickel. (a,b) Total transmission probability for the case where the substrate and tip have their magnetizations aligned parallel and anti-parallel respectively.

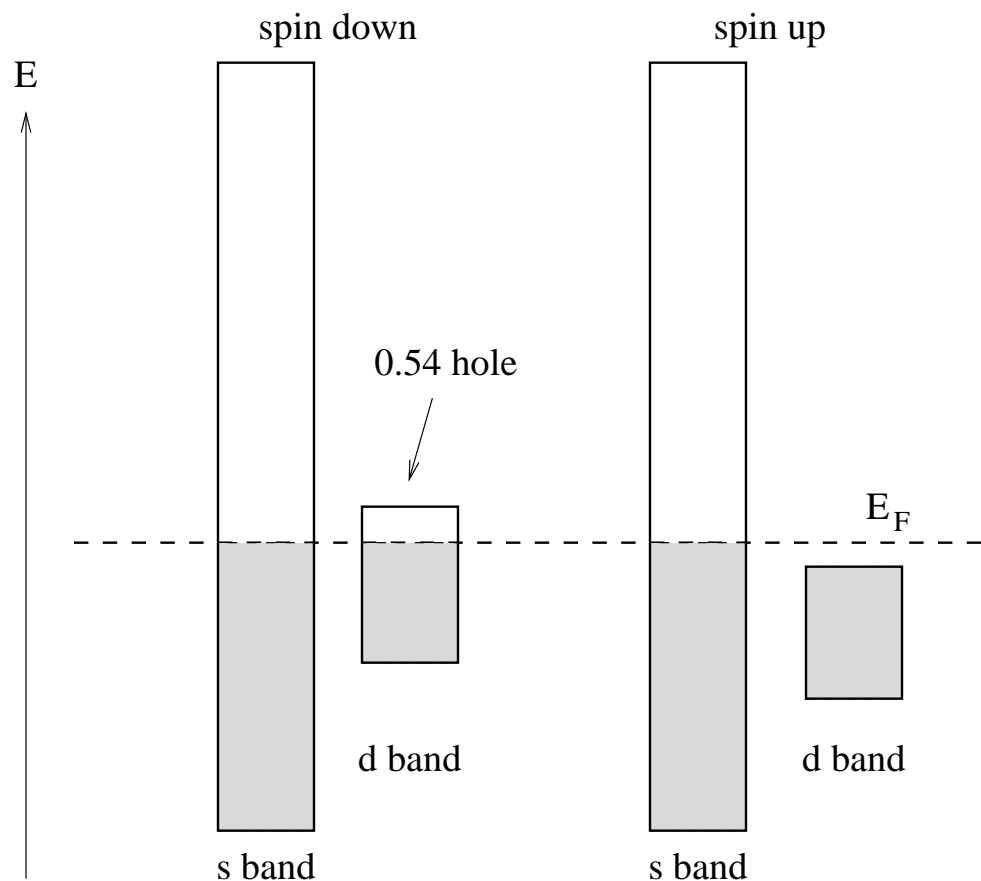
FIG. 9. Calculated differential conductance at room temperature for the Ni STM tip - BT - Ni substrate system, using a Fermi energy of -8.5 eV. (Solid line) STM tip and substrate magnetizations aligned parallel, (dashed line) aligned anti-parallel.



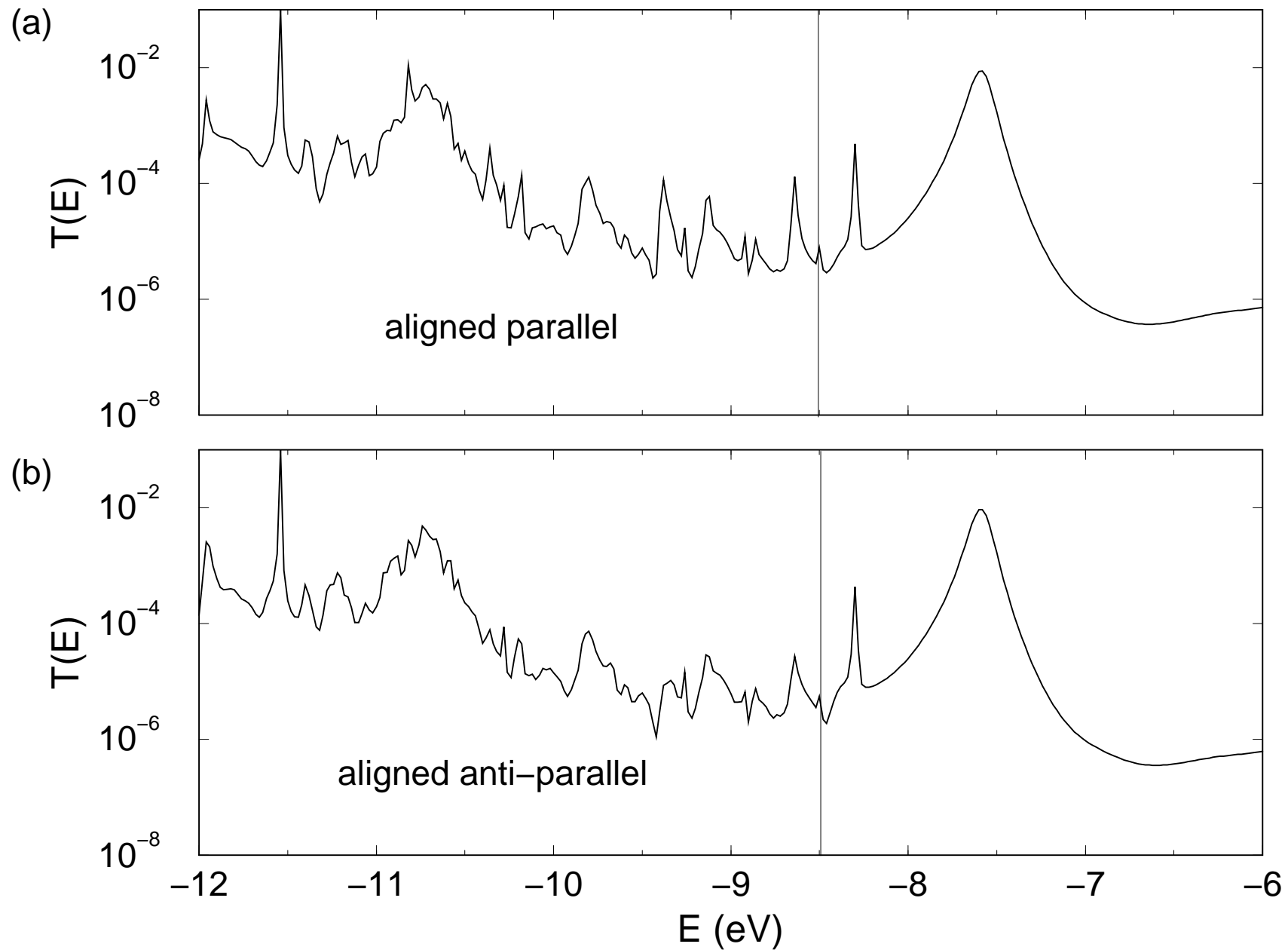


Emberly & Kirczenow Fig. 2

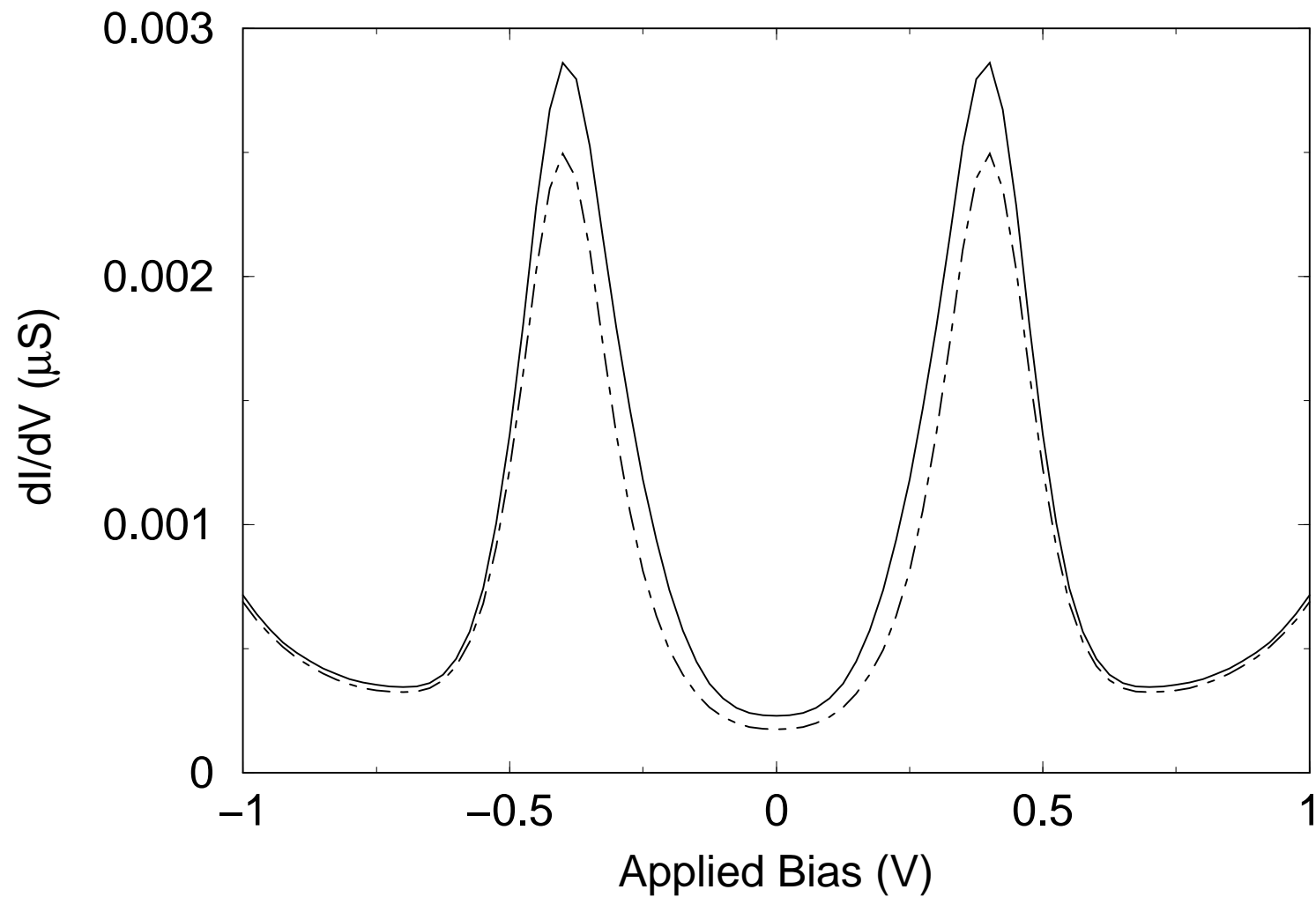
Nickel Band Structure



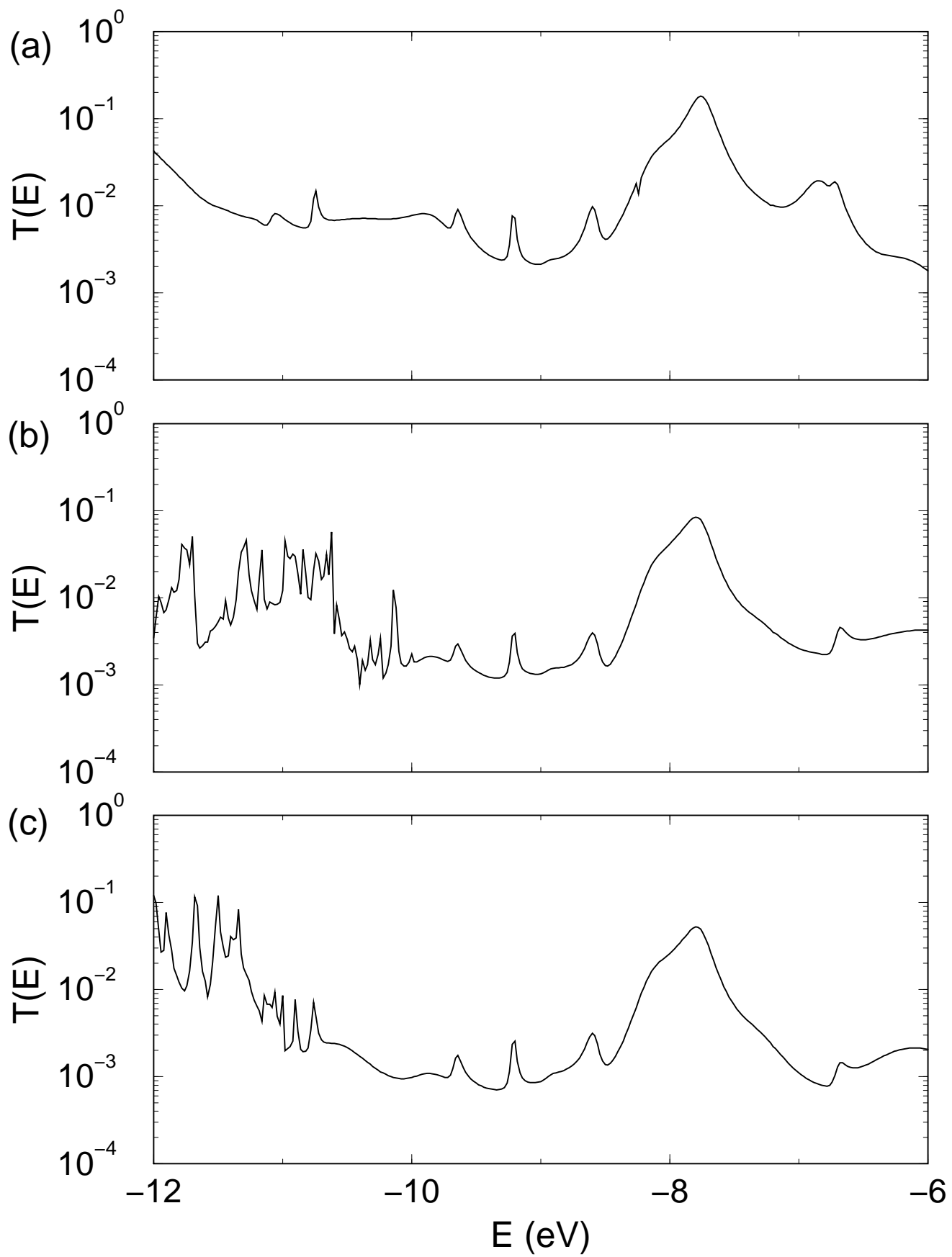
Emberly & Kirczenow Fig.3



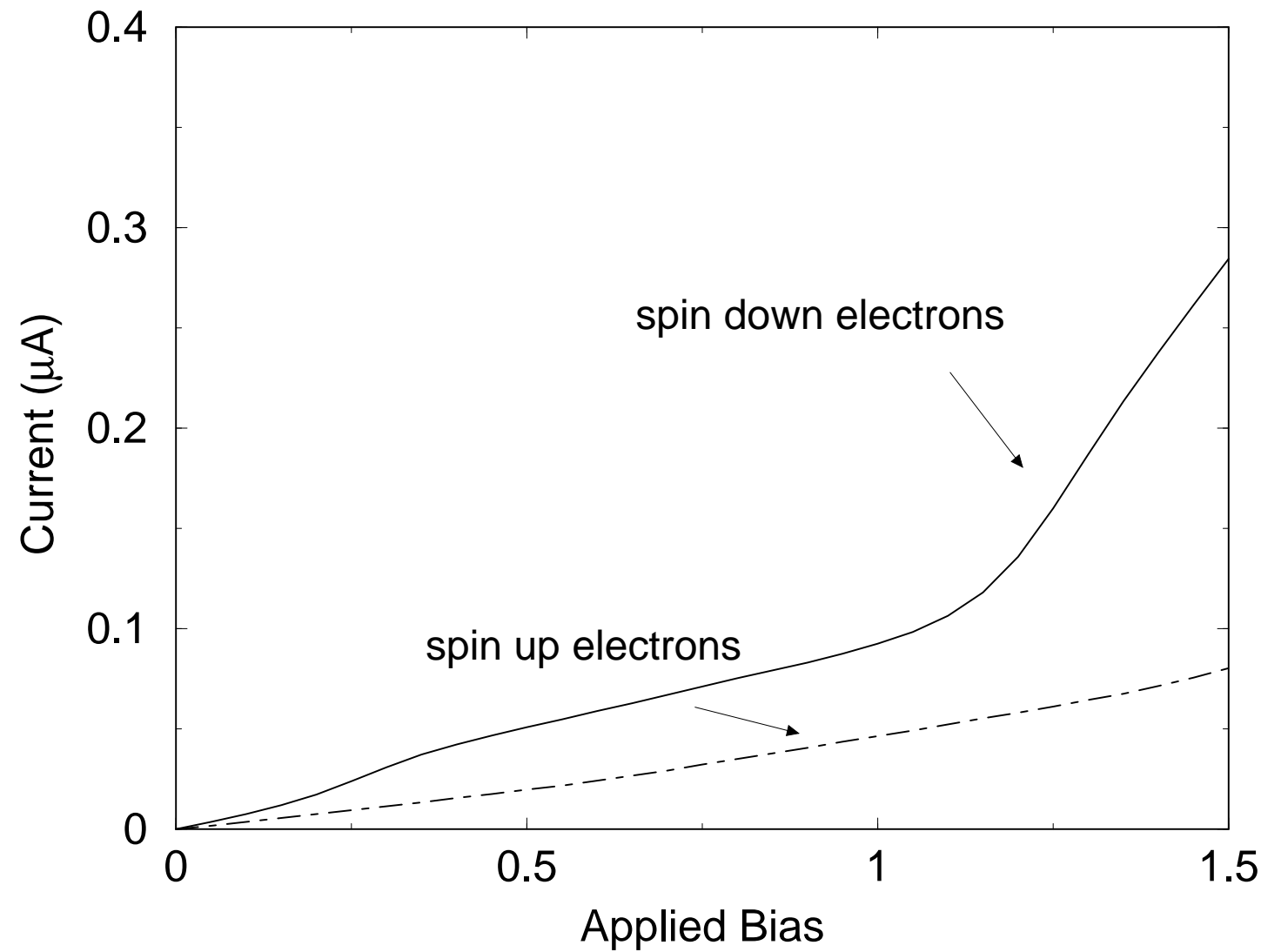
Emberly & Kirczenow Fig. 4



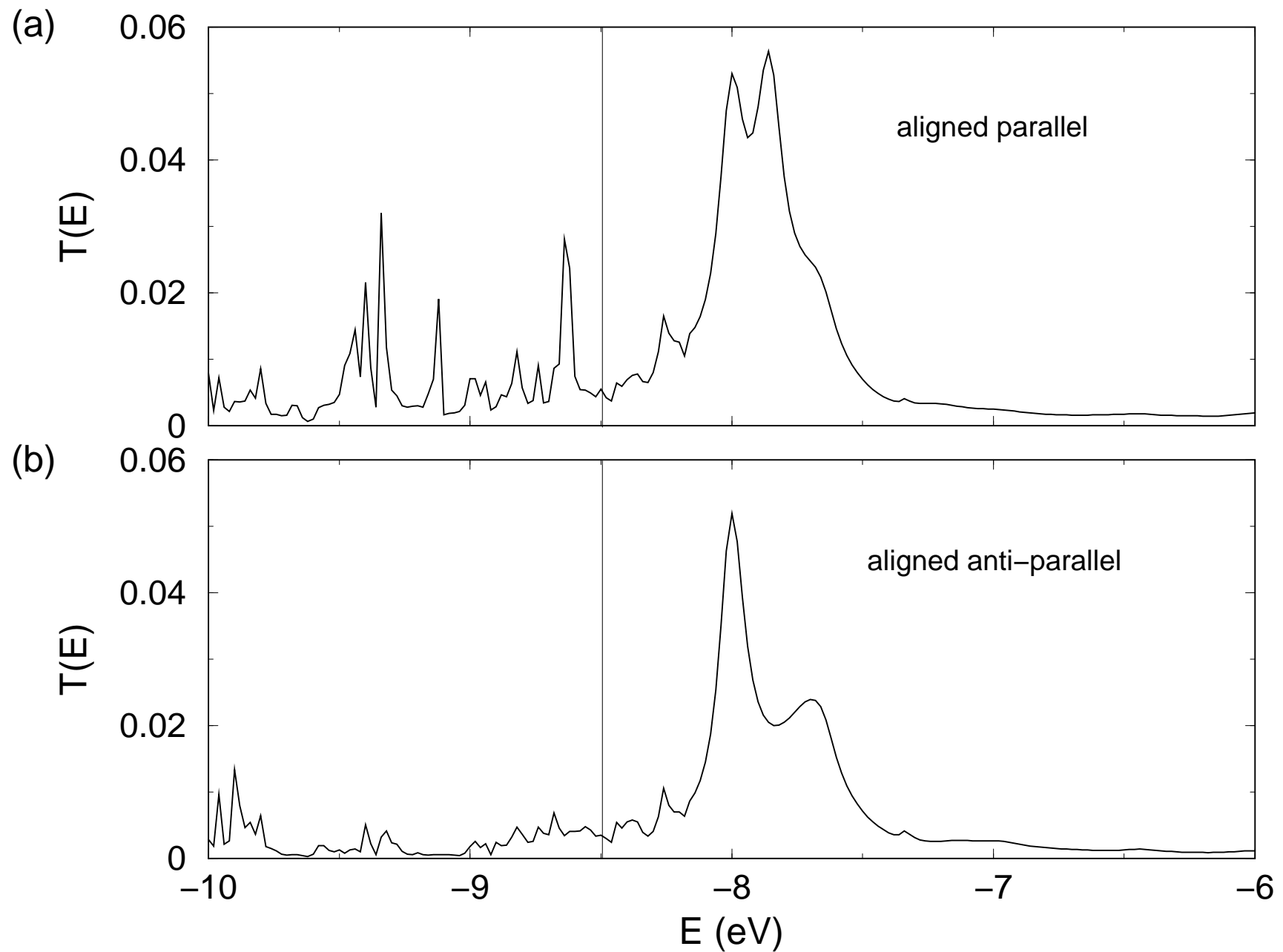
Emberly & Kirczenow Fig. 5



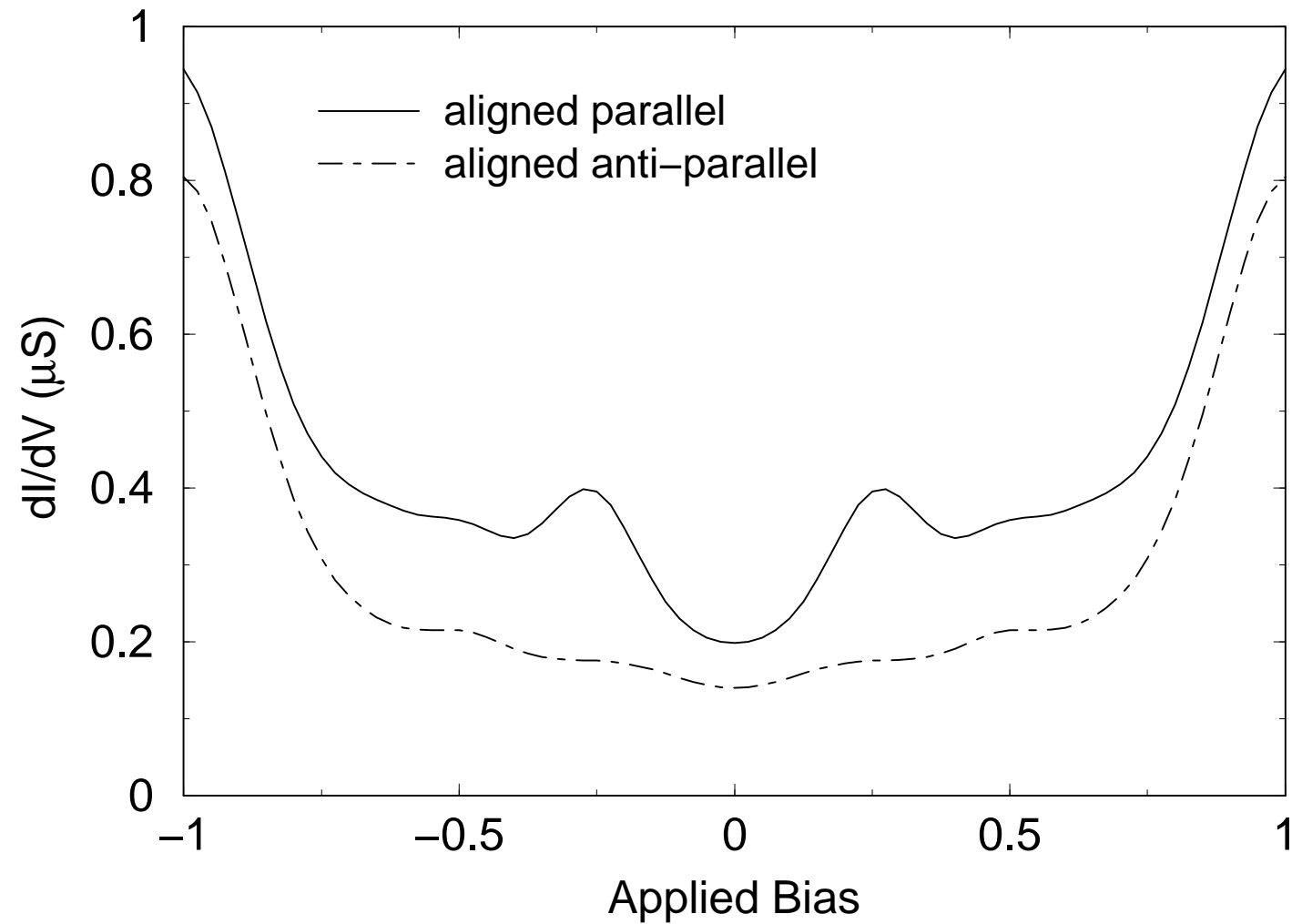
Emberly & Kirczenow Fig. 6



Emberly & Kirczenow Fig. 7



Emberly & Kirczenow Fig. 8



Emberly & Kirczenow Fig. 9